Dynamics of the Einstein–de Haas effect: Application to a magnetic cantilever

Reem Jaafar, E. M. Chudnovsky, and D. A. Garanin
Department of Physics, Lehman College, City University of New York, 250 Bedford Park Boulevard West, Bronx, New York 10468-1589, USA

(Received 17 November 2008; revised manuscript received 26 January 2009; published 11 March 2009)

The local time-dependent theory of Einstein–de Haas effect is developed. We begin with microscopic interactions and derive dynamical equations that couple elastic deformations with internal twists due to spins. The theory is applied to the description of the motion of a magnetic cantilever caused by the oscillation of the domain wall. Theoretical results are compared with a recent experiment on the Einstein–de Haas effect in a microcantilever.

DOI: 10.1103/PhysRevB.79.104410 PACS number(s): 75.80.+q, 72.55.+s, 07.55.Jg

I. INTRODUCTION

The Einstein–de Haas effect[1] consists of the mechanical rotation of a freely suspended body, caused by the change in its magnetic moment. The latter can be induced by, e.g., the applied magnetic field or by rapid warming. The Einstein–de Haas effect is a direct consequence of the conservation of the total angular momentum (spin+orbital). Consider, e.g., a solid made of N atoms of magnetic moment $\mathbf{M}=\gamma_J\mathbf{J}$, where $\mathbf{J}=\mathbf{S}+\mathbf{L}$ is the operator of the total angular momentum of the atom (that includes spin $\mathbf{S}$ and orbital moment $\mathbf{L}$) and $\gamma_J=g_Je/2mc$ is the gyromagnetic ratio for J, where $e<0$ is the charge of electron and $g_J=1+[2J(J+1)]^{-1}[J(J+1)+S(S+1)-L(L+1)]$ is the Lande factor. The total angular momentum of the magnet suspended from a string is a sum of $N\langle\mathbf{J}\rangle$ and the mechanical orbital moment $\boldsymbol{\mathcal{L}}$ due to the rotation of the solid. If, for example, the solid, initially nonmagnetized and at rest, develops a macroscopic magnetic moment $\boldsymbol{\mathcal{M}}=N\langle\mathbf{M}\rangle=\gamma_JN\langle\mathbf{J}\rangle$, then the conservation law requires that $N\langle\mathbf{J}\rangle+\mathcal{L}=0$. This gives $\boldsymbol{\mathcal{L}}=-\boldsymbol{\mathcal{M}}/\gamma_J$, that is, the solid begins to rotate on being magnetized.

Experiments on the Einstein–de Haas effect and the related Barnett effect[2] (generation of the magnetic moment by mechanical rotation), performed at the dawn of quantum physics, provided first measurements of the gyromagnetic ratio for various materials.[3] Even today the Einstein–de Haas method can still provide a more accurate value of g_J as compared to electron-spin resonance and ferromagnetic resonance methods that require precise knowledge of the effective magnetic field inside the sample.[4] Nevertheless fundamental questions about the Einstein–de Haas effect remain unanswered. In particular, the global conservation of the angular momentum does not explain how the angular momentum is actually transferred from individual atoms to the whole body. This question is clearly related to the magnetic relaxation and decoherence at the atomic level. The latter determines the width of para- and ferromagnetic resonances, as well as functionality of spin-based qubits. Advances in manufacturing and measuring of nanomechanical devices promise to revive interest in the local dynamics of the Einstein–de Haas effect.

Our interest in this problem has been ignited by a recent experiment performed at the National Institute of Standards and Technology (NIST) laboratory in Boulder, Colorado.[5] In that experiment a 50 nm Permalloy film was deposited onto a $200\times20\times0.6$ μm^3 cantilever. The cantilever was placed inside a coil that generated an ac magnetic field. Oscillation of the cantilever was measured by a fiber-optic interferometer positioned above the tip of the cantilever. When the frequency of the ac field matched the resonance frequency of the cantilever the amplitude of the oscillations was about 3 nm. The data were analyzed within a model that replaced the mechanical torque due to change in the magnetization with the effect of the periodic force acting on the fictitious point mass at the free end of the cantilever. Such an approximation, while catching some features of the phenomenon, is clearly insufficient for the study of the microscopic dynamics of the Einstein–de Haas effect.

In this paper we will develop the theoretical framework for the description of the dynamics of the Einstein–de Haas effect that we will apply to the problem of the magnetic cantilever. To make this problem more transparent we shall assume (as is the case for many magnetic solids) that the magnetism is of spin origin and can be described either by individual spins $\mathbf{S}_i$, localized at the atomic sites i, or by a continuous spin field $\mathbf{S}(\mathbf{r},t)$. (Generalization to magnetism of spin and/or orbital origin can be obtained through a straightforward redefinition of the constants.) We shall derive general equations describing the transfer of the spin angular momentum to the mechanical angular momentum of the body. In the NIST experiment the length of the cantilever was large compared to the thickness of the domain wall. Consequently, the effect of the ac magnetic field was likely to change the magnetization of the Permalloy film through the motion of the domain wall separating two magnetic domains inside the film. We shall pay special attention to this case. The cantilever problem will be solved by adding the internal torque due to the motion of the domain wall to the equations of the elastic theory describing the motion of the cantilever. The obtained dynamics of the cantilever is rather rich and it allows a detailed comparison between theory and experiment.

The general theory of spin-rotation coupling will be studied in Sec. II. Equations of the elastic theory with internal twists due to the dynamics of spins will be derived in Sec. III. Mechanical motion of the magnetic cantilever will be studied in Sec. IV. Suggestions for experiments will be given in Sec. V.

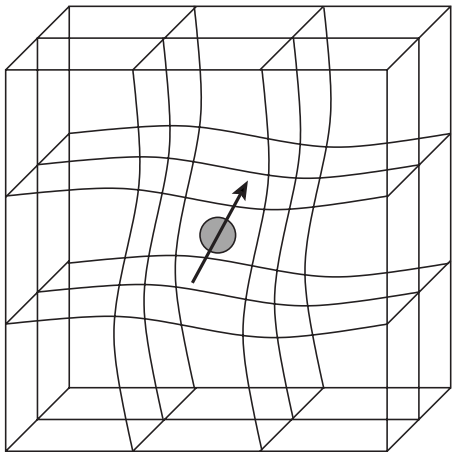

FIG. 1. Rotation of the crystal field due to local elastic twist at the location of the spin.

II. MICROSCOPIC THEORY OF SPIN-ROTATION COUPLING

Spin-lattice interaction comes from magnetostriction and spin-rotation coupling. Only the latter, however, is responsible for the Einstein–de Haas effect. The most obvious effect of local elastic twists comes from the dependence of the energy of a spin on its orientation in the crystal-magnetic anisotropy. This effect is due to spin-orbit interactions and is of relativistic origin. It is described by the crystal-field Hamiltonian that can be very generally written as

$$\hat{H}_A = \sum_j K_j^{\alpha\beta} S_j^\alpha S_j^\beta + \sum_j L_j^{\alpha\beta\gamma\delta} S_j^\alpha S_j^\beta S_j^\gamma S_j^\delta + \cdots . \tag{1}$$

Here the Greek letters denote Cartesian components of a dimensionless spin vector $\mathbf{S}_j$ belonging to the site j of the crystal lattice. Tensors, $K_j^{\alpha\beta}, L_j^{\alpha\beta\gamma\delta}, \ldots$, describing magnetic anisotropy, are defined in the coordinate frame $\mathbf{e}_j^{(1,2,3)}$ that is rigidly coupled to the locally defined crystal axes (see Fig. 1). Local rotation of the lattice is performed by the (3×3) rotation matrix $\mathbb{R}_j$,

$$\mathbf{e}_j^{(1,2,3)} \to \mathbb{R}_j \mathbf{e}_j^{(1,2,3)}. \tag{2}$$

It results in

$$K_j^{\alpha\beta} \to \mathbb{R}_j^{\alpha\gamma}\mathbb{R}_j^{\beta\delta} K_j^{\gamma\delta},$$

$$L_j^{\alpha\beta\gamma\delta} \to \mathbb{R}_j^{\alpha\eta}\mathbb{R}_j^{\beta\xi}\mathbb{R}_j^{\gamma\theta}\mathbb{R}_j^{\delta\epsilon} L_j^{\eta\xi\theta\epsilon} \cdots . \tag{3}$$

For a small rotation at the site j by an angle $\delta\phi_j$, one has

$$\mathbb{R}_j^{\alpha\beta} = \delta^{\alpha\beta} - \epsilon^{\alpha\beta\gamma}\delta\phi_j^\gamma. \tag{4}$$

We now notice that due to the rotational invariance of $\hat{H}_A$, the rotation of the local frame $(\mathbf{e}_j^{(1)}, \mathbf{e}_j^{(2)}, \mathbf{e}_j^{(3)})$ is equivalent to the rotation of the vector $\mathbf{S}_j$ by the same angle in the opposite direction, $\mathbf{S} \to \mathbb{R}^{-1}\mathbf{S}$. As it is known,[6] this rotation can be equivalently performed by the $(2S+1)\times(2S+1)$ matrix in the spin space,

$$\mathbf{S}_j \to \hat{R}_j \mathbf{S}_j \hat{R}_j^{-1}, \quad \hat{R}_j = e^{-i\mathbf{S}_j\cdot\delta\phi_j}. \tag{5}$$

Consequently, in the presence of rotations, $\hat{H}_A$ becomes[7,8]

$$\hat{H}_A' = \hat{R}\hat{H}_A\hat{R}^{-1}, \tag{6}$$

where

$$\hat{R} = \exp\left(-i\sum_j \mathbf{S}_j\cdot\delta\phi_j\right). \tag{7}$$

In the linear order on $\delta\phi_j$ one obtains

$$\hat{R}\hat{H}_A\hat{R}^{-1} \cong \hat{H}_A + \hat{H}_R, \quad \hat{H}_R = i\sum_j [\hat{H}_A, \mathbf{S}_j]\cdot\delta\phi_j. \tag{8}$$

By quantizing $\delta\phi_j$ one can apply this Hamiltonian to the study of rigid spin clusters and quantum dots.[9–11]

The total spin Hamiltonian $\hat{H}_S$ may include exchange interaction, magnetostriction, Zeeman interaction, and dipole-dipole interaction. The dipole-dipole interaction is usually the weakest one and will not be considered here. The magnetostriction is local on spin. Consequently, it is transformed by rotations the same way as the crystal field. The Zeeman interaction of spins with the external magnetic field $\mathbf{B}$,

$$\hat{H}_Z = \sum_j \mathbf{b}\cdot\mathbf{S}_j, \quad \mathbf{b} \equiv g\mu_B\mathbf{B}, \tag{9}$$

is not affected by rotations; g is the gyromagnetic factor for the spin. Here we take into account that the magnetic moment due to spin, $\mathbf{M}=-g\mu_B\mathbf{S}$, has direction opposite to $\mathbf{S}$ because of the negative gyromagnetic ratio for the electron. Finally, the exchange interaction

$$\hat{H}_{\rm ex} = -\frac{1}{2}\sum_{ij} I_{ij}\mathbf{S}_i\cdot\mathbf{S}_j \tag{10}$$

only depends on the local arrangement of spins that is not affected by rotations. In the first order on $\delta\phi_j$, the generalization of Eq. (8) is

$$\hat{H}_R = i\sum_j [\hat{H}_S, \mathbf{S}_j]\cdot\delta\phi_j - i\sum_j [(\hat{H}_Z + \hat{H}_{\rm ex}), \mathbf{S}_j]\cdot\delta\phi_j. \tag{11}$$

The last two terms appeared in Eq. (11) because the Zeeman Hamiltonian (9) and the exchange Hamiltonian (10) that are included in $\hat{H}_S$ are independent from local rotations. Consequently, one should subtract $\hat{H}_Z$ and $\hat{H}_{\rm ex}$ from $\hat{H}_S$ when computing the effect of rotations.

Let the total Hamiltonian of the system that incorporates all couplings, including interactions with rotations, be $\hat{H}$. It is clear that the difference between $[\hat{H}_S, \mathbf{S}_j]$ and $[\hat{H}, \mathbf{S}_j]$ begins with the terms that are linear on $\delta\phi_j$. Thus, in the linear approximation on $\delta\phi_j$, we can replace $i[\hat{H}_S, \mathbf{S}_j]$ in Eq. (11) with $i[\hat{H}, \mathbf{S}_j] = \hbar\dot{\mathbf{S}}_j$. Working out the commutator with the Zeeman Hamiltonian in Eq. (11) one obtains

$$\hat{H}_R = \sum_j \left(\hbar\dot{\mathbf{S}}_j + \mathbf{S}_j\times\mathbf{b} - i\sum_j [\hat{H}_{\rm ex}, \mathbf{S}_j]\right)\cdot\delta\phi_j. \tag{12}$$

III. ELASTIC THEORY WITH INTERNAL TWISTS DUE TO SPIN-ROTATION COUPLING

Our approach to the Einstein–de Haas effect is based on Eq. (12). To apply this equation to the long-wave torsional deformations of the body we shall write $\delta\phi_j$ in terms of the displacement field of the elastic theory $\mathbf{u}(\mathbf{r},t)$,[12]

$$\delta\phi(\mathbf{r}) = \frac{1}{2}\nabla \times \mathbf{u}(\mathbf{r}), \tag{13}$$

and replace $\mathbf{S}_j$ with the spin density $\mathbf{S}(\mathbf{r},t)$. The classical energy of the body then becomes

$$\mathcal{H} = \mathcal{H}_S + \mathcal{H}_E + \mathcal{H}_R. \tag{14}$$

Here $\mathcal{H}_E$ is the elastic energy of the body written in terms of $\mathbf{u}(\mathbf{r},t)$ while $\mathcal{H}_S = \langle H_S \rangle$ includes exchange, anisotropy, Zeeman and dipolar energies, magnetostriction, etc., written in terms of $\mathbf{S}(\mathbf{r},t)$ and $\mathbf{u}(\mathbf{r},t)$.[13] The last term in Eq. (14) follows from Eqs. (12) and (13),

$$\mathcal{H}_R = \frac{1}{2}\int d^3r[\hbar\dot{\mathbf{S}} + \mathbf{S}\times(\mathbf{b}+\mathbf{b}_{\rm ex})]\cdot(\nabla\times\mathbf{u}), \tag{15}$$

where[13]

$$\mathbf{b}_{\rm ex} = \frac{\delta\mathcal{H}_{\rm ex}}{\delta\mathbf{S}} = -I_{\alpha\beta}\frac{\partial^2\mathbf{S}}{\partial r_\alpha\,\partial r_\beta} \tag{16}$$

and

$$I_{\alpha\beta} = \frac{1}{2}\sum_j I_{ij}(r_i^\alpha - r_j^\alpha)(r_i^\beta - r_j^\beta). \tag{17}$$

The dynamical equation for the displacement field is[12]

$$\rho\frac{\partial^2 u_\alpha}{\partial t^2} = \frac{\partial\sigma_{\alpha\beta}}{\partial x_\beta}, \tag{18}$$

where $\sigma_{\alpha\beta} = \delta\mathcal{H}/\delta e_{\alpha\beta}$ is the stress tensor, $e_{\alpha\beta} = \partial u_\alpha/\partial x_\beta$ is the strain tensor, and ρ is the mass density of the material. The stress tensor can be divided into two parts, $\sigma_{\alpha\beta} = \sigma_{\alpha\beta}^{(\rm M)} + \sigma_{\alpha\beta}^{(\rm R)}$, with

$$\sigma_{\alpha\beta}^{(\rm M)} = \frac{\delta(\mathcal{H}_S + \mathcal{H}_E)}{\delta e_{\alpha\beta}} \tag{19}$$

and

$$\sigma_{\alpha\beta}^{(\rm R)} = \frac{\delta\mathcal{H}_R}{\delta e_{\alpha\beta}}. \tag{20}$$

Here $\sigma_{\alpha\beta}^{(\rm M)}$ is the mechanical part of the stress tensor, e.g., the part coming from the elastic properties of the cantilever plus magnetostriction, while $\sigma_{\alpha\beta}^{(\rm R)}$ is the part of the stress tensor produced by the internal rotations due to spins,

$$\sigma_{\alpha\beta}^{(\rm R)} = -\frac{1}{2}\epsilon_{\alpha\beta\gamma}\{\hbar\dot{S}_\gamma + [\mathbf{S}\times(\mathbf{b}+\mathbf{b}_{\rm ex})]_\gamma\}. \tag{21}$$

Notice that, contrary to the symmetric stress tensor ($\sigma_{\alpha\beta} = \sigma_{\beta\alpha}$) used by the conventional elastic theory, $\sigma_{\alpha\beta}^{(\rm R)}$ is antisymmetric. The immediate consequence of that is a nonzero torque,

$$dK_{\alpha\beta}^{(\rm R)} = (\sigma_{\alpha\beta} - \sigma_{\beta\alpha})d^3r, \tag{22}$$

acting on the volume element d^3r. Such torques, neglected by the conventional theory of elasticity, are responsible for the Einstein–de Haas effect.

Equations (18)–(21) allow one to obtain the general dynamical equation of the elastic theory that accounts for local internal forces due to the dynamics of spins in a ferromagnet as follows:

$$\rho\frac{\partial^2 u_\alpha}{\partial t^2} - \frac{\partial\sigma_{\alpha\beta}^{(\rm M)}}{\partial x_\beta} = f_\alpha^{(\rm R)}, \tag{23}$$

where

$$\mathbf{f}^{(\rm R)} = -\frac{1}{2}\boldsymbol{\nabla}\times[\hbar\dot{\mathbf{S}} + \mathbf{S}\times(\mathbf{b}+\mathbf{b}_{\rm ex})]. \tag{24}$$

Let us check that these equations conserve the total angular momentum (spin+orbital). Writing the total angular momentum due to the spins and the crystal as

$$\mathbf{J} = \int d^3r[\hbar\mathbf{S} + \rho(\mathbf{r}\times\dot{\mathbf{u}})], \tag{25}$$

one obtains the following equation for the time derivative of the αth component of $\mathbf{J}$:

$$\begin{aligned}\dot{J}_\alpha &= \int d^3r[\hbar\dot{S}_\alpha + \epsilon_{\alpha\beta\gamma}r_\beta(\rho\ddot{u}_\gamma)] \\ &= \int d^3r\Bigg\{\hbar\dot{S}_\alpha + \epsilon_{\alpha\beta\gamma}r_\beta\nabla_\delta\sigma_{\gamma\delta}^{(\rm M)} - \frac{1}{2}[r_\beta\nabla_\alpha - (\mathbf{r}\cdot\boldsymbol{\nabla})\delta_{\alpha\beta}] \\ &\quad\times[\hbar\dot{S}_\beta + (\mathbf{S}\times\mathbf{b})_\beta - \epsilon_{\beta\gamma\delta}I_{\epsilon\eta}S_\gamma\nabla_\epsilon\nabla_\eta S_\delta]\Bigg\},\end{aligned} \tag{26}$$

where we have used Eqs. (16), (23), and (24). If one prohibits the transfer of spin angular momentum through the surface, integration by parts with account of the symmetry of $\sigma_{\alpha\beta}^{(\rm M)}$ and $I_{\alpha\beta}$ gives

$$\dot{\mathbf{J}} = \mathbf{K}^{(\rm M)} + \mathbf{K}^{(\rm R)} \tag{27}$$

with

$$K_\alpha^{(\rm M)} = \int dA_\delta[\epsilon_{\alpha\beta\gamma}r_\beta\sigma_{\gamma\delta}^{(\rm M)}] \tag{28}$$

and

$$\mathbf{K}^{(\rm R)} = \int d^3r(\mathbf{b}\times\mathbf{S}). \tag{29}$$

Here $\mathbf{K}^{(\rm M)}$ is the external mechanical torque applied to the surface of the body $\mathbf{A}$, while $\mathbf{K}^{(\rm R)}$ is the volume spin torque due to the external magnetic field. Thus, in accordance with our expectation, when external forces are absent, Eq. (23) conserves the total angular momentum, $\dot{\mathbf{J}} = 0$.

If the spin-lattice interaction were absent there would be no deformation induced by the dynamics of spins. This condition provides another check of the validity of Eqs. (23) and (24). In the absence of dissipation the spin field satisfies[13]

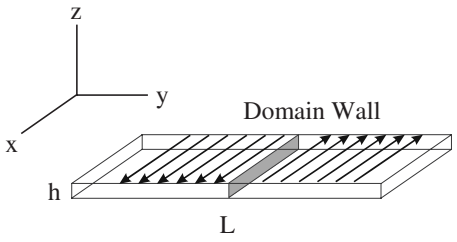

FIG. 2. Geometry considered in the paper.

$$\hbar\dot{\mathbf{S}} = -\mathbf{S}\times\mathbf{b}_{\text{eff}}, \tag{30}$$

where $\mathbf{b}_{\text{eff}}=\delta\mathcal{H}/\delta\mathbf{S}$ is the effective field that can be presented as $\mathbf{b}_{\text{eff}}=\mathbf{b}+\mathbf{b}_{\text{ex}}+\mathbf{b}'$. Here $\mathbf{b}'$ is determined by the spin-lattice coupling. Its main part is usually the anisotropy field, $\mathbf{b}_A=\delta\mathcal{H}_A/\delta\mathbf{S}$. Equations (23) and (30) then show that Zeeman and exchange interactions alone do not provide any force on the body. This is in accordance with the fact that spins should couple to the lattice in order to produce such a force. Dissipation can be incorporated into the problem by adding standard damping terms to the elastic equation (23) and Landau-Lifshitz equation (30).

IV. DYNAMICS OF MAGNETIC CANTILEVER

Among many problems involving internal forces due to spins, Eq. (23) can be used for computation of the elastic motion of a magnetic cantilever. For example, in the case of the motion of a domain wall inside the cantilever, one substitutes the known domain-wall solution for $\mathbf{S}(\mathbf{r},t)$ into the right-hand side of Eq. (23), while the left-hand side follows from the elastic theory of the cantilever in the absence of spins.[12] Sudden increase in the external magnetic field should result in the domain wall sweeping the cantilever, thus providing a source of deformation during a finite time. Application of a harmonic ac magnetic field, as in the NIST experiment, should lead to the oscillation of the position of the domain wall inside the cantilever.

The geometry of the problem is shown in Fig. 2. The cantilever of length L, parallel to the Y direction, is magnetized in the X direction. The $y=0$ end of the cantilever is attached to the holder while the $y=L$ end is free. We are interested in small displacements of the cantilever in the Z direction, $u_z(y,t)$, caused by the time-dependent external magnetic field. Vectors $\mathbf{B}$ and $\mathbf{S}$ are assumed to lie in the XY plane. The latter property of the magnetization is common for thin films. It is easy to see that in this case the terms proportional to $\mathbf{S}\times\mathbf{b}$ and $\mathbf{S}\times\mathbf{b}_{\text{ex}}$ in the right-hand side of Eq. (23) give zero contribution to the Z component of the elastic equation. Adding the term proportional to $\dot{\mathbf{S}}$ to the right-hand side of the conventional equation of motion for a cantilever,[12] one obtains from Eq. (23)

$$\rho\frac{\partial^2 u_z}{\partial t^2}+\frac{h^2E}{12(1-\sigma^2)}\frac{\partial^4 u_z}{\partial y^4}=\frac{\hbar}{2}\frac{\partial}{\partial y}\frac{\partial}{\partial t}S_x(y,t), \tag{31}$$

where h is the thickness of the cantilever in the Z direction, E is the Young's modulus, and σ is the Poisson coefficient $(-1<\sigma<1/2)$.

If the magnetization of the cantilever was rotating uniformly in space, then according to Eq. (31) the force from spins would only act on the free end of the cantilever where the magnetization has a discontinuity. However, for a soft magnetic material such as Permalloy, deposited on a cantilever that is large compared to the dimensions of a monodomain particle, the change in the magnetization should occur through the motion of a domain wall. For that reason we shall describe the magnetic state of the cantilever by two domains separated by the domain wall at $y=y_0(t)$. In what follows we will neglect the back effect of the motion of the cantilever on the domain wall.[14] This assumption is justified by the calculation below that shows that the displacement of the cantilever caused by the motion of the domain wall is always very small. Then $S_x(y,t)$ is given by the conventional domain-wall solution centered at $y=y_0(t)$,

$$S_x(y,t)=S_{\text{dw}}[y-y_0(t)]. \tag{32}$$

In the absence of the dc magnetic field this gives

$$\rho\frac{\partial^2 u_z}{\partial t^2}+\frac{h^2E}{12(1-\sigma^2)}\frac{\partial^4 u_z}{\partial y^4}=-\frac{\hbar}{2}\left(\frac{dy_0}{dt}\right)\frac{\partial^2}{\partial y^2}S_{\text{dw}}[y-y_0(t)]. \tag{33}$$

For the dissipative motion of the domain wall the speed of the wall is proportional to the field. When the ac magnetic field $B=B_0\cos(\omega t)$ is applied in the X direction, one has $y_0(t)=y_0(0)+a\sin(\omega t)$, where $a<L$ is the amplitude of the oscillations around $y_0(0)$. The domain wall is given by $S_{\text{dw}}(y,t)=S_0F[y-y_0(t)]$, where S_0 is a constant spin density and F changes from -1 to $+1$ as one crosses the wall. Note the connection of S_0 to the magnetization, $M_0=g\mu_BS_0$.

It is convenient to switch to dimensionless variables

$$\bar{u}_z=\frac{u_z}{L},\quad \bar{y}=\frac{y}{L},\quad \bar{t}=t\nu,\quad \nu\equiv\sqrt{\frac{Eh^2}{12\rho(1-\sigma^2)L^4}}, \tag{34}$$

where L is the length of the cantilever and ν determines the scale of the eigenfrequencies of its vertical oscillations, $u_z(y,t)$. In terms of these variables Eq. (33) becomes

$$\frac{\partial^2\bar{u}_z}{\partial\bar{t}^2}+\frac{\partial^4\bar{u}_z}{\partial\bar{y}^4}=-\epsilon\left(\frac{d\bar{y}_0}{d\bar{t}}\right)\frac{\partial^2F}{\partial\bar{y}^2}, \tag{35}$$

where

$$\epsilon=\frac{\hbar S_0}{2\rho L^2\nu}=\frac{\hbar S_0}{2\rho}\sqrt{\frac{12\rho(1-\sigma^2)}{Eh^2}} \tag{36}$$

is a dimensionless parameter that does not depend on the length of the cantilever L. By order of magnitude, $\epsilon\sim\hbar/Msh$, where $M\sim\rho/S_0$ is the mass of the material per spin 1/2 and $s\sim\sqrt{E/\rho}$ is the speed of sound. It is easy to see that ϵ is a small parameter that can hardly exceed 0.01 even for the smallest cantilevers.

For the given function $\bar{y}_0(\bar{t})$ that describes the motion of the domain wall, Eq. (35) has to be solved with the following boundary conditions:

$$\bar{u}_z = 0, \quad \frac{\partial \bar{u}_z}{\partial \bar{y}} = 0 \quad \text{at } \bar{y} = 0,$$

$$\frac{\partial^2 \bar{u}_z}{\partial \bar{y}^2} = 0, \quad \frac{\partial^3 \bar{u}_z}{\partial \bar{y}^3} = 0 \quad \text{at } \bar{y} = 1. \tag{37}$$

The first two conditions correspond to the absence of displacement and the absence of bending of the cantilever at the fixed end, while the last two conditions correspond to the absence of torque and force, respectively, at the free end.[12]

For the free oscillations of the cantilever, $\epsilon=0$, one writes

$$\bar{u}_z(\bar{y},\bar{t}) = \bar{u}(\bar{y})\cos(\bar{\omega}\bar{t}). \tag{38}$$

Substitution into Eq. (35) with $\epsilon=0$ then gives

$$\frac{\partial^4 \bar{u}}{\partial \bar{y}^4} - \kappa^4 \bar{u} = 0, \quad \kappa^2 \equiv \bar{\omega}. \tag{39}$$

The general solution of this equation is

$$\bar{u}(\bar{y}) = A\cos(\kappa\bar{y}) + B\sin(\kappa\bar{y}) + C\cosh(\kappa\bar{y}) + D\sinh(\kappa\bar{y}), \tag{40}$$

where A, B, C, and D are constants of integration. With the help of the first, second, and fourth boundary conditions (37) one obtains

$$C = -A, \quad D = -B, \quad B = \frac{\sin\kappa - \sinh\kappa}{\cos\kappa + \cosh\kappa} A. \tag{41}$$

Substitution of these expressions into Eq. (40) gives up to a normalization factor

$$\bar{u}(\bar{y}) = (\cos\kappa + \cosh\kappa)[\cos(\kappa\bar{y}) - \cosh(\kappa\bar{y})] + (\sin\kappa - \sinh\kappa)[\sin(\kappa\bar{y}) - \sinh(\kappa\bar{y})]. \tag{42}$$

The third of the boundary conditions (37) provides an equation,

$$\cos\kappa\cosh\kappa + 1 = 0, \tag{43}$$

for the frequencies of the normal modes of the cantilever, $\bar{\omega}_n = \kappa_n^2$ [measured in the units of ν of Eq. (34)]. The fundamental (minimal) frequency is $\bar{\omega}_1 \approx 3.516$. The next two frequencies are $\bar{\omega}_2 \approx 22.03$ and $\bar{\omega}_3 \approx 61.70$. The profiles of the oscillations of the cantilever for three normal modes ($n=1,2,3$) are shown in Fig. 3.

We shall now turn to the forced oscillations of the cantilever due to motion of the domain wall. We first neglect dissipation and write for the displacement

$$\bar{u}_z(\bar{y},\bar{t}) = \sum_m R_m(\bar{t})\bar{u}_m(\bar{y}), \tag{44}$$

where $R_m(t)$ are functions of time to be determined and $\bar{u}_m(\bar{y})$ are normalized eigenfunctions (42) of the free cantilever that correspond to eigenvalues κ_m given by Eq. (43),

$$\int_0^1 d\bar{y}\, \bar{u}_m(\bar{y})\bar{u}_n(\bar{y}) = \delta_{mn}. \tag{45}$$

Substitution of Eq. (44) into Eq. (35) gives

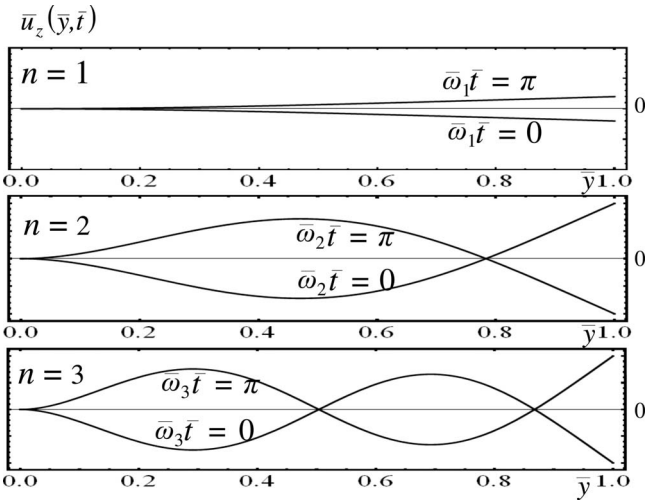

FIG. 3. Profiles of the oscillating cantilever at different moments of time for $n=1,2,3$.

$$\sum_m \left(\frac{d^2 R_m}{d\bar{t}^2} + \bar{\omega}_m^2 R_m\right)\bar{u}_m(\bar{y}) = -\epsilon\left(\frac{d\bar{y}_0}{d\bar{t}}\right)\frac{\partial^2 F}{\partial \bar{y}^2}, \tag{46}$$

where we have used Eq. (39). Multiplying both parts of this equation by $\bar{u}_n(\bar{y})$ and integrating over $\bar{y}$ from 0 to 1 with account of Eq. (45), one obtains a linear second-order differential equation for $R_n(\bar{t})$,

$$\frac{d^2 R_n}{d\bar{t}^2} + \bar{\omega}_n^2 R_n = -\epsilon\left(\frac{d\bar{y}_0}{d\bar{t}}\right)\int_0^1 d\bar{y}\frac{\partial^2 F}{\partial \bar{y}^2}\bar{u}_n(\bar{y}). \tag{47}$$

When the width of the domain wall is small compared to the length of the cantilever, the first derivative of F can be replaced with the δ function,

$$\frac{\partial F}{\partial \bar{y}} = 2\delta[\bar{y} - \bar{y}_0(\bar{t})]. \tag{48}$$

In this case, integrating by parts in the right-hand side of Eq. (47), one obtains

$$\frac{d^2 R_n}{d\bar{t}^2} + \bar{\omega}_n^2 R_n = 2\epsilon\left(\frac{d\bar{y}_0}{d\bar{t}}\right)\left(\frac{d\bar{u}_n}{d\bar{y}}\right)_{\bar{y}=\bar{y}_0(\bar{t})} = -2\epsilon\frac{d}{d\bar{t}}\bar{u}_n[\bar{y}_0(\bar{t})]. \tag{49}$$

Dissipation can be included into the problem by adding the first time derivative of R_n to this equation. This results in a following conventional problem of damped oscillations induced by a periodic force:

$$\frac{d^2 R_n}{d\bar{t}^2} + \frac{\bar{\omega}_n}{Q_n}\frac{dR_n}{d\bar{t}} + \bar{\omega}_n^2 R_n = -2\epsilon\frac{d}{d\bar{t}}\bar{u}_n[\bar{y}_0(\bar{t})]. \tag{50}$$

Here Q_n is the quality factor of the oscillations of the cantilever at the eigenfrequency $\bar{\omega}_n$.

The most interesting case is when the position of the domain wall,

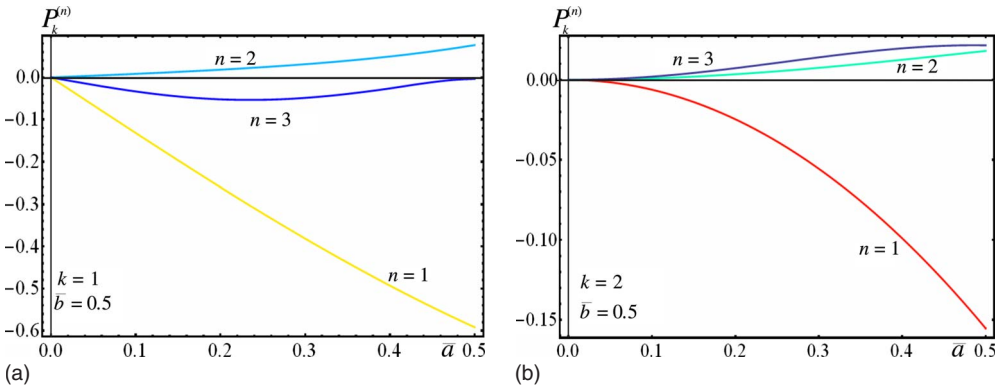

FIG. 4. (Color online) The dependence of $P_k^{(n)}(\bar{a},\bar{b})$ on the amplitude of the oscillations of the domain wall whose equilibrium position is in the middle of the cantilever: (a) $k=1$ and (b) $k=2$.

$$\bar{y}_0(\bar{t}) = \bar{b} + \bar{a}\,\sin(\bar{\omega}\bar{t}), \tag{51}$$

oscillates at a frequency $\bar{\omega}$ that is close to one of the resonant frequencies of the cantilever $\bar{\omega}_n = \kappa_n^2$. To solve Eq. (50) we write u_n and R_n as Fourier series,

$$u_n(\bar{t}) = \sum_{k=-\infty}^{\infty} u_k^{(n)} e^{ik\bar{\omega}\bar{t}}, \quad R_n(\bar{t}) = \sum_{k=-\infty}^{\infty} r_k^{(n)} e^{ik\bar{\omega}\bar{t}}. \tag{52}$$

Substitution into Eq. (50) gives

$$r_k^{(n)} = \frac{-2i\epsilon k\bar{\omega}u_k^{(n)}}{\bar{\omega}_n^2 - k^2\bar{\omega}^2 + \dfrac{ik\bar{\omega}\bar{\omega}_n}{Q_n}}, \tag{53}$$

where

$$u_k^{(n)}(\bar{a},\bar{b}) = \frac{1}{2\pi}\int_0^{2\pi} d\xi\, e^{-ik\xi}\bar{u}_n(\bar{b} + \bar{a}\,\sin\,\xi). \tag{54}$$

Writing $u_k^{(n)}$ as $u_k^{(n)} = |u_k^{(n)}|\exp[i\gamma_k^{(n)}]$ one obtains the following expressions for the amplitude $|r_k^{(n)}|$ and phase $\delta_k^{(n)}$ of the kth harmonic of $R_n(t)$:

$$|r_k^{(n)}| = \frac{2\epsilon k\bar{\omega}|u_k^{(n)}|}{\sqrt{(k^2\bar{\omega}^2 - \bar{\omega}_n^2)^2 + \left(\dfrac{k\bar{\omega}\bar{\omega}_n}{Q_n}\right)^2}}, \tag{55}$$

$$\delta_k^{(n)} = \gamma_k^{(n)} - \frac{\pi}{2} + \arctan\left[\frac{k\bar{\omega}\bar{\omega}_n}{Q_n(k^2\bar{\omega}^2 - \bar{\omega}_n^2)}\right]. \tag{56}$$

According to Eq. (55), resonances occur at frequencies $\omega = \omega_n/k$ that are independent of damping. At $\omega = \omega_n/k$ the maximum displacement of the free end of the cantilever is given by

$$\bar{u}_z(1) = \epsilon Q_n P_k^{(n)}(\bar{a},\bar{b}), \tag{57}$$

where

$$P_k^{(n)}(\bar{a},\bar{b}) = \frac{2\bar{u}_n(1)}{\bar{\omega}_n}|u_k^{(n)}(\bar{a},\bar{b})|. \tag{58}$$

The dependence of $P_k^{(n)}$ on $\bar{a}$ and $\bar{b}$ for various k and n is illustrated in Figs. 4 and 5.

Note the nonmonotonic dependence of the amplitude of the free end on the equilibrium position of the domain wall for $n=2$ and $n=3$. It is due to the profile of the normal modes of the cantilever shown in Fig. 3. When the equilibrium position of the wall coincides with the antinode, the effect of the oscillation of the wall on the cantilever is minimal.

V. SUGGESTIONS FOR EXPERIMENT

Expressions derived in this paper provide the framework for theoretical analysis of the experimental data on the

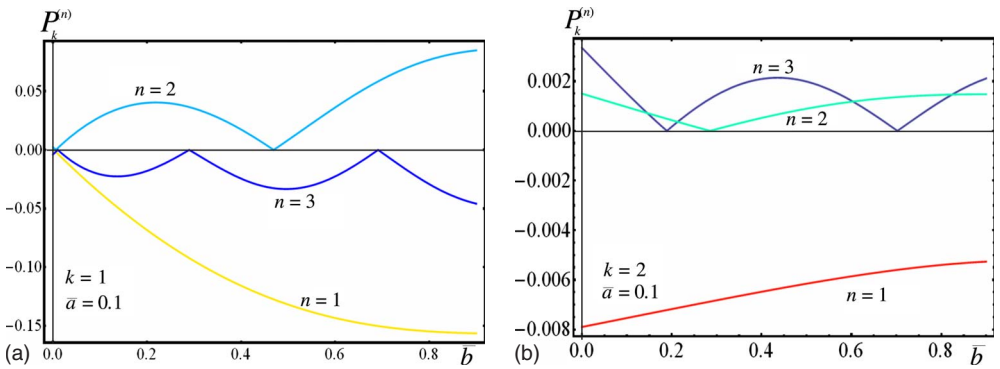

FIG. 5. (Color online) The dependence of $P_k^{(n)}(\bar{a},\bar{b})$ on the equilibrium position of the domain wall for $n=1,2,3$ and $k=1,2$.

Einstein–de Haas effect. To illustrate the applications of the theory we have derived rigorous formulas for the mechanical motion of a magnetic cantilever, induced by the motion of a domain wall when the cantilever is placed in the ac magnetic field. In our theory we assumed that the entire volume of the cantilever was magnetic. The formulas can be easily adjusted, however, to the situation when the magnetic layer has thickness $ph<h$, as was the case in the NIST experiment. In this case the strength of the source in the right-hand side of Eq. (35) reduces by the factor p. Consequently, one should replace ϵ in the above formulas with $\epsilon_p=p\epsilon<\epsilon$.

Accurate comparison between theory and experiment requires precise knowledge of the mechanism by which the magnetic moment is changing. If it is due to the motion of the domain wall, as we believe was the case in the NIST experiment,[5] then one needs to know the initial equilibrium position b and the amplitude of the oscillations of the wall a. They can be measured by, e.g., combining the optical detection of the displacement of the cantilever[5] with the Faraday rotation technique, as well as by magnetic force[15] and Lorentz microscopy. The parameter b can be controlled by a weak dc magnetic field, while a can be controlled by the amplitude of the ac field. It is also desirable to excite various harmonics ω_n/k and to identify the fundamental frequency ω_1. This would allow one to obtain the value of the parameter ν in Eqs. (34) and (36). If the magnetization and the g factor are known, the ratio S_0/ρ in the first of Eq. (36) can be computed with good accuracy. The precision with which the parameter ϵ can be determined will then depend on the knowledge of the length of the cantilever L. Alternatively, ϵ can be extracted from experiment and used to obtain the spin density S_0. If the magnetization M_0 is known this would allow one to obtain the gyromagnetic factor $g=M_0/\mu_B S_0$.

In the NIST experiment the fraction of the magnetic material p was close to 1/12 while the dimensions of the cantilever were $L=2\times10^{-4}$ m and $h=6\times10^{-7}$ m. This gives $\epsilon_p\sim10^{-7}$. If a is comparable to L, then according to Eq. (57), the deflection of the free end of the cantilever at the fundamental frequency $\omega=\omega_1$ must be on the order of $\epsilon_p Q_1 L$. The observed deflection in the nanometer range then corresponds to $Q_1\sim100$. We should notice in this connection that the effect could be stronger for a cantilever with a higher quality factor. As a matter of fact the quality factors as high as 10 000 have been reported for microcantilevers.[16,17] For a cantilever of length $L=0.2$ mm such a high-quality factor would allow the deflection of the free end due to the Einstein–de Haas effect as high as a few tens of a micrometer.

So far we have studied the classical motion of the cantilever caused by the classical motion of the domain wall. Our general equations, however, are based on quantum theory and apply to the quantum dynamics as well. Solution of the problem that studies the quantized states of a nanomagnet entangled with the mechanical states of the cantilever will be reported elsewhere.

ACKNOWLEDGMENT

This work was supported by the NSF under Grant No. DMR-0703639.

[1] A. Einstein and W. J. de Haas, Verh. Dtsch. Phys. Ges. **17**, 152 (1915); **18**, 173 (1916); **18**, 423 (1916).
[2] S. J. Barnett, Phys. Rev. **6**, 239 (1915).
[3] See, e.g., V. Ya. Frenkel', Sov. Phys. Usp. **22**, 580 (1979) about the history of Einstein–de Haas and Barnett experiments.
[4] S. J. Barnett and G. S. Kenny, Phys. Rev. **87**, 723 (1952); G. G. Scott and H. W. Sturner, *ibid.* **184**, 490 (1969), and references therein.
[5] T. M. Wallis, J. Moreland, and P. Kabos, Appl. Phys. Lett. **89**, 122502 (2006).
[6] A. Messiah, *Quantum Mechanics*, Lecture Notes in Physics Vol. 2 (Wiley, New York, 1976).
[7] V. Dohm and P. Fulde, Z. Phys. B **21**, 369 (1975).
[8] E. M. Chudnovsky, D. A. Garanin, and R. Schilling, Phys. Rev. B **72**, 094426 (2005).
[9] E. M. Chudnovsky and D. A. Garanin, Phys. Rev. Lett. **93**, 257205 (2004).
[10] C. Calero, E. M. Chudnovsky, and D. A. Garanin, Phys. Rev. Lett. **95**, 166603 (2005).
[11] C. Calero and E. M. Chudnovsky, Phys. Rev. Lett. **99**, 047201 (2007).
[12] L. D. Landau and E. M. Lifshitz, *Theory of Elasticity* (Pergamon, New York, 1959).
[13] See, e.g., E. M. Chudnovsky and J. Tejada, *Lectures on Magnetism* (Rinton, Princeton, NJ, 2006).
[14] A. A. Kovalev, G. E. W. Bauer, and A. Brataas, Phys. Rev. Lett. **94**, 167201 (2005).
[15] K. C. Fong, P. Banerjee, Yu. Obukhov, D. V. Pelekhov, and P. C. Hammel, arXiv:0805.0266 (unpublished).
[16] E. K. Irish and K. Schwab, Phys. Rev. B **68**, 155311 (2003).
[17] E. Finot, A. Passian, and T. Thundat, Sensors **8**, 3497 (2008).